https://www.sciencedirect.com/science/article/pii/S0048969717322283

Seasonal variability of $PM_{2.5}$ and PM_{10} composition and sources in an urban background site in Southern Italy

Author links open overlay panel

D.Cesari[a] G.E.De Benedetto[b] P.Bonasoni[c] M.Busetto[c] A.Dinoi[a] E.Merico[a] D.Chirizzi[b] P.Cristofanelli[c] A.Donateo[a] F.M.Grasso[a] A.Marinoni[c] A.Pennetta[b] D.Contini[a]

https://doi.org/10.1016/j.scitotenv.2017.08.230

Highlights

- Composition and sources of $PM_{2.5}$ and $PM_{2.5-10}$ are investigated in South-eastern Italy.
- Secondary organic and inorganic components were 43% of $PM_{2.5}$ with opposite seasonal trends.
- Two forms of nitrate were observed: sodium nitrate and ammonium nitrate (only in winter).

- PMF and mass-closure identified two soil sources accounting for 29% of $PM_{2.5–10}$.

- Biomass burning is an important source at the urban background site even during warm seasons.

Abstract

Comparison of fine and coarse fractions in terms of sources and dynamics is scarce in southeast Mediterranean countries; differences are relevant because of the importance of natural sources like sea spray and Saharan dust advection, because most of the monitoring networks are limited to PM_{10}. In this work, the main seasonal variabilities of sources and processes involving fine and coarse PM (particulate matter) were studied at the Environmental-Climate Observatory of Lecce (Southern Italy). Simultaneous $PM_{2.5}$ and PM_{10} samples were collected between July 2013 and July 2014 and chemically analysed to determine concentrations of several species: OC (organic carbon) and EC (elemental carbon) via thermo-optical analysis, 9 major ions via IC, and 23 metals via ICP-MS. Data was processed through mass closure analysis and Positive Matrix Factorization (PMF) receptor model characterizing seasonal variabilities of nine sources contributions. Organic and inorganic secondary aerosol accounts for 43% of $PM_{2.5}$ and 12% of $PM_{2.5–10}$ with small seasonal changes. SIA (secondary inorganic aerosol) seasonal pattern is opposite to that of SOC (secondary organic carbon). SOC is larger during the cold period, sulphate (the major contributor to SIA) is larger during summer.

Two forms of nitrate were identified: $NaNO_3$, correlated with chloride depletion and aging of sea-spray, mainly present in $PM_{2.5–10}$; NH_4NO_3 more abundant in $PM_{2.5}$. Biomass burning is a relevant source with larger contribution during autumn and winter because of the influence of domestic heating, however, is not negligible in spring and summer, because of the contributions of fires and agricultural practices. Mass closure analysis and PMF results identify two soil sources: crustal associated to long range transport and carbonates associated to local resuspended dust. Both sources contributes to the coarse fraction and have different dynamics with crustal source contributing mainly in high winds from SE conditions and carbonates during high winds from North direction.

Graphical abstract

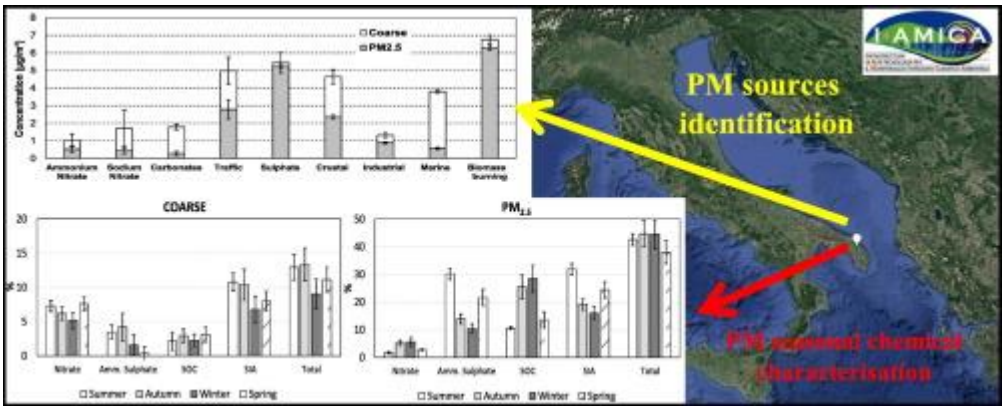

1. Download : Download high-res image (435KB)
2. Download : Download full-size image

- Previous article in issue

- Next article in issue

Keywords

PM2.5PM10Source apportionmentSeasonal variabilitiesSecondary aerosolChloride depletion

1. Introduction

Particulate matter (PM) is one of the most studied atmospheric pollutant due to its potential effects on local and regional air quality, on visibility, and on global climate (Fuzzi et al., 2015). Moreover, there is a compelling evidence that exposure to PM leads to adverse health effects including respiratory and cardiovascular diseases, allergies, and premature mortality (Pope et al., 2004, Delfino et al., 2005, Dockery and Stone, 2007, Gauderman et al., 2015, Velali et al., 2016). Current studies indicate that $PM_{2.5}$ (particles with an aerodynamic diameter smaller than 2.5 μm) was responsible in 2010 of over 3 million premature deaths per year worldwide and 11.5% of these premature deaths are concentrated in Europe (Jerret, 2015, Lelieveld et al., 2015).

Atmospheric PM concentrations in Mediterranean basin are influenced by air masses coming from Europe, Eastern Countries and Africa (Lelieveld et al., 2002). Mediterranean Sea is bordered by 21 Countries accounting for > 400 million inhabitants (in 2011), mostly concentrated near the coasts (Salameh et al., 2015). Being delimited at North by highly industrialised southern Europe Countries and by Africa in the South, PM concentrations are affected by a number of natural and anthropogenic sources such as road traffic, biomass burning, shipping, Saharan dust advection, and sea spray (Viana et al., 2014, Contini et al., 2014a, Salameh et al., 2015, Amato et al., 2016, Merico et al., 2017). Mediterranean region is also characterised by complex meteorology that favours aging of polluted air masses (Artíñano et al., 2001). This plays an important role in formation of secondary particles and in their successive aging with a high degree of oxidation of the organic aerosol (Hildebrandt et al., 2011).

Recent results of the AIRUSE project (Amato et al., 2016) evidenced that the spatial variability and the sources of $PM_{2.5}$ in southern Europe are less known with respect to PM_{10} because the fine fraction is not widely measured. As a consequence, there is also limited information on spatial and temporal variability of coarse fraction ($PM_{2.5–10}$), often linked to local and natural sources, being an increasing concern for health (Brunekreef and Forsberg, 2005). Therefore, further research efforts are needed to investigate long-term trends of sources of fine and coarse PM fractions in this area for air quality applications, for management of health risks, and for analysis of PM impact to climate change in Mediterranean basin.

This work analyses the first year (between summer 2013 and summer 2014) of simultaneous measurements of $PM_{2.5}$ and PM_{10} concentrations and chemical compositions collected at the Environmental-Climate Observatory, recently built in South-Est Italy (in Lecce), regional station of the Global Atmosphere Watch (GAW) network. Chemical composition is studied evaluating the concentrations of nine major water-soluble ions, of 23 metals including elements of crustal and anthropogenic origin, and evaluating the carbon content. Carbonaceous species were determined separating elemental carbon (EC) mainly of primary origin from combustion sources, and organic carbon (OC) having a primary and a secondary component. Chemical composition was used for mass closure analysis and for application of Positive Matrix Factorization (PMF) receptor model to investigate seasonal variabilities of the contributions of the main natural and anthropogenic sources to fine ($PM_{2.5}$) and coarse size fractions. Seasonal variabilities of secondary organic and inorganic aerosol concentrations were investigated, including their correlation with local meteorology, to improve the understanding of the main chemical and physical processes governing the dynamics of PM in this area.

2. Experimental

2.1. Measurement station and sampling

PM_{10} and $PM_{2.5}$ daily samples were collected at the Environmental-Climate Observatory of Lecce (Fig. S1), regional station of the GAW-WMO network (Global Atmosphere Watch, see Cristofanelli et al., 2016). The Observatory is located in south-eastern Italy (40°20′8″N–18°07′28″E) at 37 m a.s.l. inside the University Campus of Lecce. The station could be characterised as urban background because it is not strongly influenced by traffic or industrial emissions (Chirizzi et al., 2017). In this site, pollution levels are not significantly influenced by local specific sources rather by the integrated contributions of all sources upwind. The Observatory site is influenced by the activities (included traffic) inside the University Campus, and by the diffused emissions of the town of Lecce and of the other small villages located nearby the Campus. Moreover, the area is sometimes downwind of the largest industrial settlements of the Apulia Region: the area of Taranto (about 80 km in the NW direction) and the area of Brindisi (about 30 km in the NNW direction).

Samples were collected daily for a one-year period between 17/07/2013 and 14/07/2014 using a low-volume (2.3 m_3/h) dual channel (one for $PM_{2.5}$ and one for PM_{10}) sequential sampler (SWAM, Fai Instruments) with automatic detection of aerosol concentration using β-ray attenuation. Particulate matter was collected on quartz filters (Whatman Q-grade, diameter 47 mm) pre-fired for 2 h at 700 °C. Mass concentration measurements with this instrument were in very good agreement with standard reference gravimetric method and the typical uncertainty on measured mass concentration was 2% on PM_{10} and 3% on $PM_{2.5}$ (Dinoi et al., 2017).

Meteorological conditions, specifically wind velocity and direction, temperature, cumulative rain, and relative humidity were obtained from the meteorological station (Vaisala WXT520) of the Observatory.

2.2. Chemical analysis

Roughly, one sample every three days was chemically analysed for a total of 226 simultaneous samples (113 for PM_{10} and 113 for $PM_{2.5}$). Each filter was divided into four quarters, three of them used for the chemical analysis and one used for quality control: replication of specific analysis.

One quarter of the filter was used to obtain a punch (1 cm_2) for the determination of OC and EC concentrations via thermo-optical method (Sunset OC/EC Analyser), following the NIOSH 5040 protocol. To ensure the accuracy of the OC and EC analysis, the analyser was calibrated (multipoint) using as external standard a sucrose solution. Blank filters were also analysed to correct measured values, obtaining for OC an average contamination level of 2.1 μg/cm_2 (standard deviation ± 0.9 μg/cm_2) and negligible contamination for EC (< 0.1 μg/cm_2).

The second quarter was used for determination of water soluble ions concentrations via High Performance Ion Chromatography (Dionex DX600 IC system composed of an AS40 Autosampler, a GP50 Gradient Pump, an LC25 Chromatography Enclosure, an ED50 Conductivity detector equipped with a temperature compensated conductivity cell) with a 125 μL injection loop. The extraction was done in two steps (20 min each in ultrasonic bath) in 20 mL of ultrapure water (Milli-Q MΩ 18). Anions (Cl^-, NO_3^-, SO_4^{2-}, $C_2O_4^{2-}$) were separated using a Dionex AS4A-4 mm column coupled with IonPac AG14 guard column and 2.7 mM Na_2CO_3 and 1.0 mM $NaHCO_3$ as eluent in isocratic mode. Cations (Ca^{2+}, Na^+, K^+, NH_4^+, Mg^{2+}) were separated using a Dionex (CS12A-4 mm) column coupled with IonPac CG12A guard column and 20 mM MSA as eluent in isocratic mode. The self-regenerating suppressors (Dionex ASRS ULTRA and Dionex CSRS ULTRA II for anions and cations, respectively) were used in the electrochemical suppression mode, operating at 50 mA to convert the

eluent solution to weakly conducting water. The external standard calibration was performed using single anions and cations solutions at 1000 mg/L (Inorganic Ventures). The laboratory control sample (LCS) was prepared adding an analytes standard solution to pre-fired filters (and successively analysed) once every 20 samples. The method detection limits (MDLs) were obtained as three times the standard deviation of the signal of blanks pre-fired filter measurements (n = 10), divided by the slope of the calibration curve. The MDLs values (μg/L) were as follows: 10.2 (Na^+), 6.1 (K^+), 39.9 (NH_4^+), 6.9 (Ca^{2+}), 2.0 (Mg^{2+}), 4.9 (Cl^-), 8.2 (NO_3^-), 140 (SO_4^{2-}), and 10.2 ($C_2O_4^{2-}$). Accuracy and precision tests were performed, for Cl^-, Na^+, K^+, Ca^{2+} and Mg^{2+}, using certified material of fly ash (NIST SRM 1648a) and, for the other ions, on pre-fired quartz filters spiked with NH_4^+, NO_3^-, SO_4^{2-} and $C_2O_4^{2-}$. The values of relative standard deviation (RSD%) were < 8% while the recovery values were between 88% (Ca^{2+}) and 108% ($C_2O_4^{2-}$).

The third quarter of filter was used to determine metals concentrations via ICP-MS (Thermo X Series II). Each sample was microwave digested in closed Teflon vessels using a two steps procedure (Aldabe et al., 2013). In the first step the sample was digested in 3 mL HF + 3 mL H_2O_2 + 1 mL HCl + 4 mL HNO_3 with the following temperature program: from room temperature up to 180 °C in 15 min, dwell time of 15 min, up to 210 °C in 15 min and a final dwell time of 15 min. The samples were then cooled overnight and evaporated to dryness for 20 min at 500 W. In the second step after addition of 10 mL of 5% H_3BO_3, temperature was increased up to 120 °C in 20 min followed by a dwell time of 15 min and 30 min cooling. Finally, samples were diluted to 25 mL in volumetric flask using water (Milli-Q MΩ 18). The ICP-MS was tuned using a TUNE A solution (Thermo) at 10 μg/L. The sample (1 mL) was transferred into 15 mL graduate tube, 200 μL of EPA6020ISS solution at 500 μg/L (Inorganic Ventures) and 8800 μL of 2% HNO_3 solution were added, and was analysed

following US EPA 6020A guidelines. The external calibration was performed for the following elements: Al, As, Ba, Cd, Ce, Co, Cu, Dy, Fe, La, Li, Mn, Nb, Nd, Pb, Rb, Sb, Se, Sr, Th, Ti, V, Zn using EPA6020CAL and single analyte standard solutions (Inorganic Ventures). Quality control checks were performed monitoring the intensities of all internal standards for every sample analysis and analysing the laboratory control sample (LCS), in each sample batch, at a frequency of one LCS every 20 samples. The LCS were prepared by pre-fired quartz filters spiked with analytes of interest before microwave procedure. The MDLs, calculated with the same approach used for anions and cations, were between 0.89 μg/L (Al) and 0.001 μg/L (La). Metal recoveries, calculated using certified material of fly ash (NIST SRM 1648a), ranged from 85% (Pb) to 112% (La) with RSD% < 15%.

Field blanks (20 for $PM_{2.5}$ and 20 for PM_{10}) were analysed following the same procedure of the exposed samples. Concentrations of the different species were obtained after subtraction of the average level present in the blank samples. The concentration for a specific species and sample was quantified if it was larger than the standard deviation σ_B of the blank filters; otherwise, a threshold value equal to $\sigma_B/2$ was considered. In cases in which the concentration was below the MDL, or not detectable above the average variability of the field blanks, a concentration value equal to the maximum between the MDL/2 and $\sigma_B/2$ was assumed. The uncertainty for concentrations < MDL or not distinguishable from blanks were assumed to be 100%, whereas the uncertainty for quantified concentration, C_{ij}, of the sample i relative to the species j, was calculated as in Cesari et al. (2014), using the Eq. (1):

$$\Delta C_{ij} = \sigma_{Bj}/2 + h_j C_{ij}$$

The values of h_j were calculated taking into account uncertainties associated to chemical analysis and the obtained values were: 2.5% for Na^+; 6% for NH_4^+; 2.8% for K^+ and Ca^{2+}; 2.5% for Mg^{2+}; 4.5% for Cl^-; 3.1% for NO_3^-; 3.8% for SO_4^{2-}; 3% for $C_2O_4^{2-}$; 5% for OC and EC; 9% for Al, Ti, Fe,

and Sr; 5% for Sb, La, Pb, and Ce; 6% for Mn, and Rb; 7% for Dy, Cu, Zn, Nb, and Th; 4% for Ba; 8% for Nd; 13% for V and Cd; 15% for Co; 16% for Li; 22% for As; 33% for Se.

2.3. Source apportionment using Positive Matrix Factorization

The characterisation of particle sources was done using the PMF approach (Paatero and Tapper, 1994). The goal of PMF is to identify the number of factors/sources, their chemical profiles, and the amount of mass, associated with each factor/source, that contributed to measured PM concentrations. In this work, the EPA PMF5 code, based on the application of the Multilinear Engine (ME-2) was used. A single input data set was obtained pooling together fine ($PM_{2.5}$) and coarse ($PM_{2.5–10}$) chemical composition. This approach has been used in other PMF applications pooling together samples belonging to particles of different sizes (Amato et al., 2009, Contini et al., 2014b) or particles collected at different sites (Pandolfi et al., 2011, Contini et al., 2012, Cesari et al., 2016a, Cesari et al., 2016b). The approach has proven to increase the statistical significance of the analysis, although it assumes that the chemical profiles of the sources do not vary for the two size fractions. The input variables were classified using the Signal-to-Noise (S/N) criteria (Paatero and Hopke, 2003), however, the percentage of data above the detection limit was also used as complementary criterion (Amato et al., 2016, Contini et al., 2016). The species Na^+, NH_4^+, K^+, Ca^{2+}, Mg^{2+}, Cl^-, NO_3^-, SO_4^{2-}, OC, EC, Ti, V, Fe, Cu, Rb, Nb, Cd, Sb, and Pb were classified as “strong variables” and used as they are in PMF5; the species $C_2O_4^{2-}$, Al, Mn, Zn, As, Se, Sr, Ba, La, Ce, Nd, Dy, and Th as “weak variables” and a tripled uncertainty was used for them in PMF5. Li and Co were classified as “bad variable” and eliminated during application of PMF5.

The best solution for the base run was obtained using eight factors. The determination of the optimal number of factors with a reasonable physical meaning was achieved analysing the parameters IM (the maximum individual column mean), and IS (the maximum individual column standard deviation), obtained from the scaled residual matrix, together with Q-values (goodness of fit parameter). In particular, for Q-values, the solution to the system was the point where the slope of the curve showed a marked change. When the number of factors increased to a critical value, IM and IS parameters experienced a marked drop. The eight factors found have a reasonable physical interpretation and the analysis of the scaled residual are symmetrically distributed for almost all variables, meaning that the model is able to reasonably fit each chemical species.

Successively, a constrained run was performed. The constraints used were: set to zero SO_4 in nitrate profile to improve the separation between secondary inorganic components; NO_3^- pull down maximally and Na^+ pull up maximally in marine profile to improve the separation between fresh and aged sea spray as shown in Cesari et al. (2016a); K^+ pull up maximally in biomass burning profile that gave good results in source apportionment in central Italy (Contini et al., 2016). The maximum change in Q allowed for each constraint was 5% and the final dQ with respect to base run was 6.4% that is comparable with the dQ used in different PMF applications (Amato et al., 2016, Cesari et al., 2016a, Contini et al., 2016).

PMF5 results reconstruct reasonably well measured concentrations for both size fractions. The fractions unexplained by the model (i.e. the average difference between measured and reconstructed concentrations) is 3% for PM_{10} and – 3.5% for $PM_{2.5}$. The linear fit of the correlation between PM_{10} reconstructed and measured concentrations had a slope of 0.93 (± 0.05) and an intercept of 1.8 (± 1.4) $\mu g/m_3$. The same analysis for $PM_{2.5}$ gave a slope of 1.03 (± 0.03) and an intercept of 0.1 (± 0.7) $\mu g/m_3$.

The uncertainties on PMF5 estimated factor profiles and contributions were evaluated using the bootstrap method (Paatero et al., 2014). The bootstrap of the "constrained solution" (applied with 100 runs with random seed, block size suggested 23, and R = 0.6) gave a good mapping of the PMF5 solution with unmapped cases limited to 1% (for carbonates and nitrate) and to 2% for crustal with the other five profiles completely mapped. The swap between the profiles was limited to 10% for all profiles with the exclusion of carbonates.

The analysis of G-space plot performed for both the base and the constrained solutions revealed that no edges are evident suggesting that the factors found are linearly independent.

3. Discussion of measured concentrations

3.1. Seasonal variabilities of the different chemical species

The yearly average $PM_{2.5}$ concentration was 18.7 (± 11.3 standard deviation) μg/m3; the yearly average concentration of PM_{10} was 29.5 (± 19.2 standard deviation) μg/m3.

Average (± standard deviations) of measured concentrations are reported in Table S1, separating the warm (spring and summer) from the cold (autumn and winter) seasons. The statistical test of Wilcoxon-Mann-Whitney has been used to individuate the species that had statistically significant (at $p < 0.05$ probability level) different median concentrations comparing the cold seasons (with an average temperature 13.8 °C) with the warm seasons (average temperature 21.7 °C). It clearly appears that chemical species in PM_{10} and $PM_{2.5}$ could be divided into three groups. The first group includes the species EC, OC, K^+, Cl^-, NO_3^-, Sb, and Pb that had seasonal variabilities with median concentrations

larger during the cold seasons in both size fractions and species that have median concentrations larger during the cold season only in $PM_{2.5}$ (Ni, As, Rb, and Ba). These species are likely associated to combustions sources like traffic, EC, OC, Sb, and Pb (Viana et al., 2006, Pakbin et al., 2011, Pulong et al., 2017) and biomass burning, EC, OC, and K^+ (Almeida et al., 2006, Cesari et al., 2016b), to sea spray (Cl^-) (Jain et al., 2017), and to secondary nitrate (NO_3^-). The second group includes the species that presented lower median concentrations during the cold seasons in both size fractions (NH_4^+, SO_4^{2-}), only in $PM_{2.5}$ (Ti and V) or only in PM_{10} (Cr, La, and Ce). These species are associated to secondary sulphate, to crustal/road dust material (Cr, La, Ce, and Ti) (Amato et al., 2014, Landis et al., 2017) and to ship emissions (V) (Sippula et al., 2009). The third group includes species that do not have statistically significant different median concentrations in the two periods: Na, Mg, Ca, $C_2O_4^{2-}$, Li, Al, Mn, Fe, Co, Cu, Zn, Se, Sr, Nb, Cd, Nd, Dy, Th.

Concentrations of measured species represent, on average, 56% (± 9% standard deviation) of PM_{10} and 61% (± 10%) of $PM_{2.5}$. In PM_{10}, the average distribution was 2.7% (± 2.2%) EC; 19.3% (± 16.8%) OC; 18.2% (± 11.2%) sum of SO_4^{2-}, NH_4^+ and NO_3^- (species associated with secondary inorganic aerosol, SIA); 11.8% (± 9.8%) sum of the other water soluble ions; 2.1% (± 2.3%) metals. In $PM_{2.5}$, the average distribution was 3.1% (± 2.2%) EC; 26.9% (± 25.8%) OC; 22.4% (± 16.0%) sum of SO_4^{2-}, NH_4^+, and NO_3^-; 6.1% (± 3.7%) sum of the other water soluble ions; 1.9% (± 1.5%) metals.

3.2. Enrichment factors of $PM_{2.5}$ and $PM_{2.5-10}$

The crustal enrichment factors (EFs) furnish information to identify the elements that have mainly a crustal origin (L. Zhang et al., 2008). The EF compares the ratios of the atmospheric concentrations of various elements with the corresponding ratios in geological material (Watson et al., 2002).

This approach is often used together with source apportionment based on receptor models (Contini et al., 2012, Tositti et al., 2014, Amato et al., 2016, Ledoux et al., 2017) to support assumptions for receptor species and sources for which little information is available (Belis et al., 2013).

The element chosen for reference is Fe to allow comparison with a previous work in this area (Contini et al., 2010) and the upper-crust composition in Wedepohl (1995) was used as geological reference. Enrichment factors calculations were also performed using Al as reference element, leading to the same conclusions regarding the elements having mainly crustal or anthropogenic origin. The EFs were analysed following the two-threshold method defined in Cesari et al. (2012) in which EF < 10 indicates an element with relevant crustal contribution; EF > 20 indicates a likely anthropogenic origin; 10 < EF < 20 indicates a mixed origin with important contribution from both natural and anthropogenic sources.

Results are reported in Fig. 1 for both the fine and the coarse fraction, also including the relative abundances of the different chemical species in each fraction. The species Fe, Sr, and Ti, generally of crustal origin present a low EF and are mainly (> 50%) contained in the coarse fraction ($PM_{2.5–10}$). For these elements, the EFs are similar in the fine and coarse fraction; for all other elements the EFs of the coarse fraction is lower than those of the fine fraction. The elements Mn, Al, La, Ce, Ba, Nb, Nd, Rb, Co, Li, Dy and Ti have low EFs being mainly of crustal origin in both size fractions. Lanthanides occur in the order of abundance Ce > La > Nd in both size fractions as it happens in natural crustal dust (Hsu et al., 2016). There is a strong correlation (Spearman coefficient 0.75, $p < 0.05$) between Ce, La, and Nd (in both size fractions $PM_{2.5}$ and PM_{10}). The average ratio Ce/La is 2.3 (± 0.2), for both size fractions, comparable with the typical ratio (about 2) observed in crustal dust (Amato et al., 2016) confirming the mineral crustal origin of these species. V is essentially crustal in the coarse fraction

but has a relevant anthropogenic contribution in $PM_{2.5}$ (EF > 10). The anthropogenic influence on V could originate by heavy oil burning, including shipping, that was relevant in the area near the coast, especially in $PM_{2.5}$ (Viana et al., 2009, Gregoris et al., 2016, Merico et al., 2017). The elements Pb, As, Cu, Zn, Cd, Sb, and Se are enriched and likely mainly of anthropogenic origin in both size fractions. The ratio La/V in crustal particles is variable between 0.25 and 0.5 (Kamber et al., 2004). The La/V ratios observed are 0.12 (± 0.02) in both size fractions confirming a possible influence of industrial emissions of V due to heavy oil combustion (Kamber et al., 2004, Hsu et al., 2016).

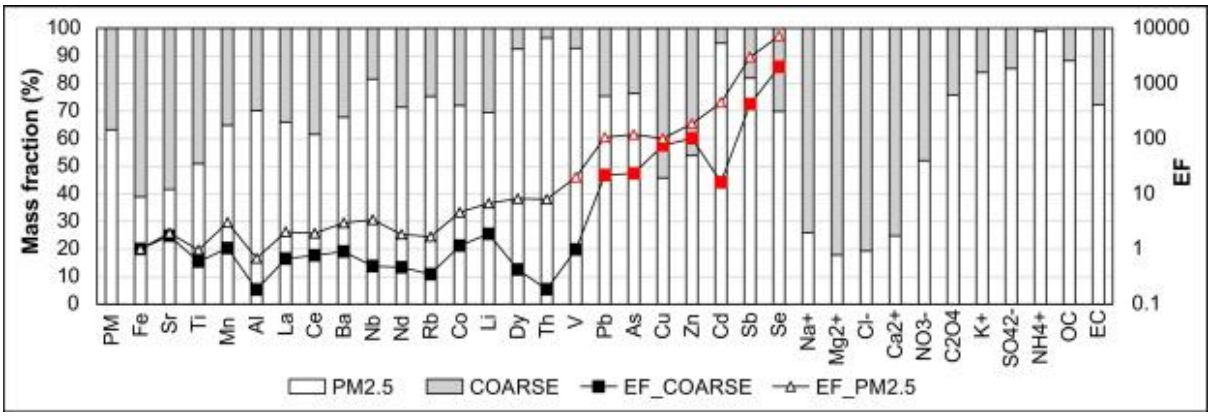

1. Download : Download high-res image (321KB)
2. Download : Download full-size image

Fig. 1

3.3. Secondary organic and inorganic aerosol

Regarding carbonaceous species, while soot has a primary origin, OC can be both primarily emitted but also formed in the atmosphere through condensation to the aerosol phase of low vapour pressure compounds emitted as primary pollutants or formed in the atmosphere (Robinson et

al., 2007, Gentner et al., 2012). Because of this, the ratio OC/EC in aerosol fractions differs widely, both in space and seasonally, and is a useful diagnostic ratio that could give information regarding the typology of the sampling sites and emission sources, and also regarding the processes happening in atmosphere which can lead to the formation of secondary organic compounds. In this study, the average OC/EC ratio was 7.8 (± 3.9) in PM_{10} and 8.8 (± 4.9) in $PM_{2.5}$, in reasonable agreement with typical ratios observed at other sites of the same typology in Italy (Sandrini et al., 2014) and in Europe (Escudero et al., 2015). However, OC/EC has a seasonal variability with a minimum value in summer of 7.7 (± 0.5) and a maximum of 11.9 (± 1.4) in winter in $PM_{2.5}$. The OC/EC ratio depends on both the proximity of the emissions and the relative weight of road traffic and biomass burning. The OC/EC ratio of road traffic emissions varies between 1.4 and 5 for gasoline catalyst vehicles and from 0.3 to 1 for diesel vehicles (Salameh et al., 2015, Amato et al., 2016). Larger values (between 5 and 12) of this ratio are generally found for biomass burning emissions (Szidat et al., 2006). The values observed at this site are larger than those associated to fossil fuel combustion and they are compatible with an urban background site located at distance from the road traffic hotspots and influenced by biomass burning especially in the cold period.

Andreae and Merlet (2001) reported values of nss-K^+/EC between 0.2 and 1.1 as typical for biomass burning and nss-K^+/EC approaching zero for fossil fuel emissions where nss-$K^+ = K^+ - 0.129Na^+$ indicates the non-sea-salt water soluble potassium. Measured nss-K^+/EC ratios in this study are significantly larger than zero: 0.14 (± 0.05) during the warm seasons and 0.29 (± 0.05) during the cold seasons, suggesting a contribution of biomass burning to EC especially during the cold seasons.

The correlation of OC with K^+ (Spearman coefficient 0.79 ($p < 0.05$) in $PM_{2.5}$ and 0.75 ($p < 0.05$) in PM_{10}) is comparable with that between OC

and EC (Spearman coefficient 0.79 ($p < 0.05$) in $PM_{2.5}$ and 0.82 ($p < 0.05$) in PM_{10}). EC is a tracer of road traffic emissions (Amato et al., 2016) while K^+ is a tracer of biomass burning emissions (Almeida et al., 2006). The correlations found suggest that both of these sources contribute to measured concentrations.

Organic matter (OM) could be evaluated as OM = 1.6OC where the factor 1.6 accounts for the non-C atoms in organic matter mass concentration (Sandrini et al., 2014). OM accounted for 31% of PM_{10} and 43% of $PM_{2.5}$. The OC/EC minimum ratio method was used to estimate the secondary organic carbon SOC concentrations (Pio et al., 2011) applying the equation:

SOC=OC−OCECminEC

The

OCECmin

ratios were determined separately for the warm and the cold periods looking at the minimum slopes (Fig. 2). The ratios for $PM_{2.5}$ were 1.6 (cold season) and 2.9 (warm season). The ratios for PM_{10} were 2.0 (cold season) and 3.3 (warm season). The differences observed between the warm and the cold seasons were likely related to the different influence of biomass burning compared to road traffic during the cold and warm seasons. This is consistent with results obtained by other studies (Shubhankar and Ambade, 2016, Blanchard et al., 2016, Zeng and Wang, 2011). SOC was mainly present in the $PM_{2.5}$ fraction, representing on average, 76% of total OC in $PM_{2.5}$ and 66% of total OC in PM_{10}. The relative share of primary (POC = OC-SOC) and secondary organic carbon in $PM_{2.5}$ has a clear seasonal variability (Fig. 3). Autumn and winter seasons have a SOC/OC ratio in $PM_{2.5}$ between 0.80 (± 0.04) and 0.86 (± 0.02) larger than the values observed during spring and summer (around 0.60 ± 0.04).

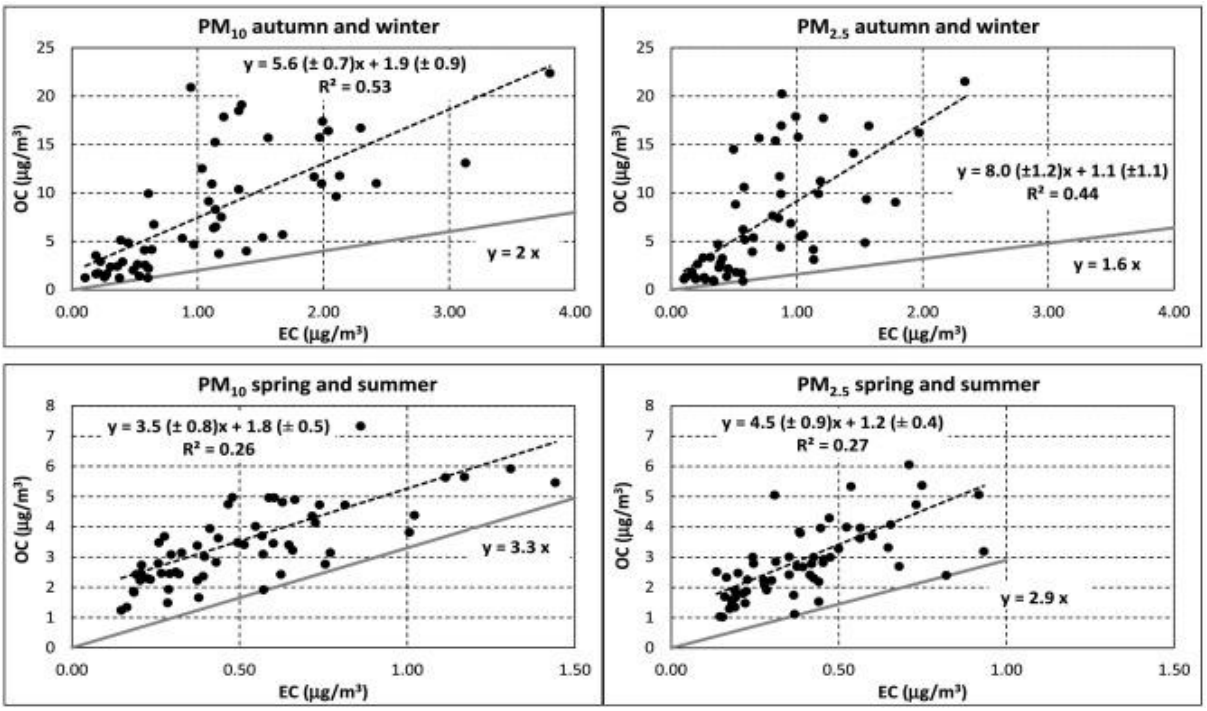

1. Download : Download high-res image (619KB)
2. Download : Download full-size image

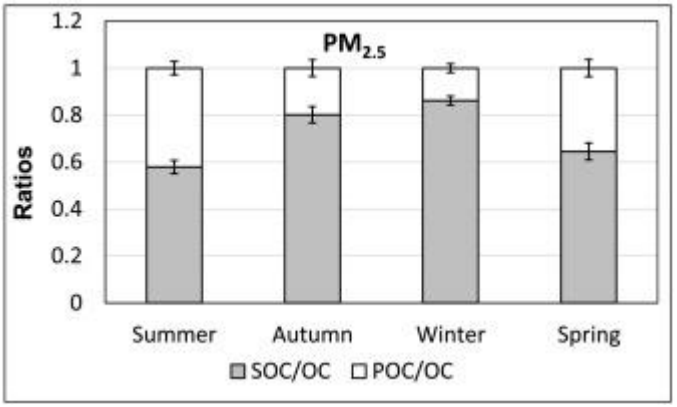

Fig. 2

1. Download : Download high-res image (98KB)
2. Download : Download full-size image

Fig. 3

The non-sea-salt sulphate was evaluated as nss-SO_{42-} = SO_{42-} – 0.25Na_{+}, it represented 91.9% of total sulphate in PM_{10} and 97.6% in $PM_{2.5}$. There is a strong correlation (Spearman coefficient 0.88 ($p < 0.05$) in $PM_{2.5}$ and 0.74 ($p < 0.05$) in PM_{10}) between SO_{42-} and NH_{4+} indicating that, on average, secondary sulphate is present as a mixture of ammonium sulphate and bisulphate. Its concentration (nss-SO_{42-} + NH_{4+}) is, on average, 3.4 μg/m_3 in $PM_{2.5}$ and 3.7 μg/m_3 in PM_{10}. The ratio nss-SO_{42-}/NH_{4+} in $PM_{2.5}$ is 2.9 near the stoichiometric ratio (2.66) expected for $(NH_4)_2SO_4$ indicating that the dominant form of secondary sulphate is, on average, ammonium sulphate.

In Fig. 4 the seasonal variability of secondary inorganic species (SIA indicates the sum of nitrate and ammonium sulphate) and SOC in fine and coarse fractions are reported. Results shows that nitrate contribution is larger on coarse fraction compared to $PM_{2.5}$, instead ammonium sulphate and SOC contribute mainly to $PM_{2.5}$. Looking at $PM_{2.5}$ fraction, there is a decrease of nitrate contribution during the warm seasons (spring and summer) because of its thermal instability (Querol et al., 2008, Pey et al., 2009) and likely for the lower NOx emissions of traffic and biomass burning during the warm period in this area (Cesari et al., 2016b). Secondary ammonium sulphate has a larger contribution during the warm seasons (spring and summer) compared to the cold seasons (autumn and winter) because the formation of ammonium sulphate is favoured at high temperatures (Querol et al., 2008, Ripoll et al., 2015). The seasonal variability of SIA follows that of ammonium sulphate which is most abundant than nitrate. In coarse fraction, nitrate contribution is similar in the different seasons and the same happens for SOC, however, ammonium sulphate is lower during winter and spring. Therefore, the total secondary contribution to the coarse fraction is relatively limited and variable between 9% (in winter) and 13% (in autumn).

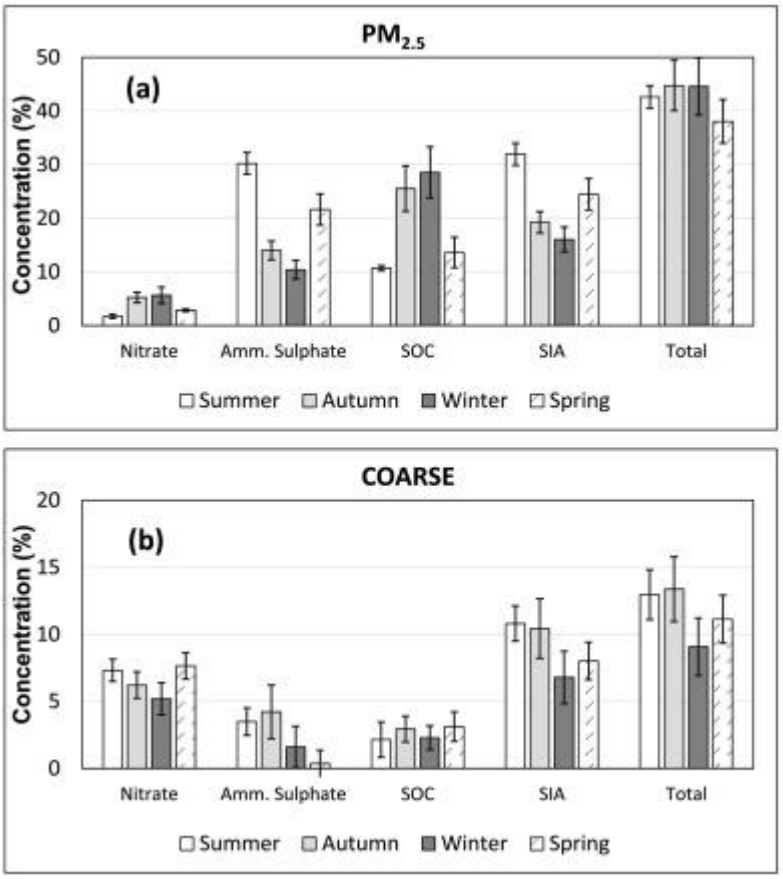

1. Download : Download high-res image (273KB)
2. Download : Download full-size image

Fig. 4

SOC has a seasonal variability opposite to that of SIA with larger concentrations during the cold period, similarly to what has been observed for OC. Low temperature favours the formation of SOC via gas-to-particle conversion of oxidized products of volatile organic compounds present in the atmosphere (Sahu et al., 2011). The opposite variabilities of SIA and SOC bring limited seasonal changes of the total secondary fraction of $PM_{2.5}$ variable between 38% during spring and 45% during autumn/winter. Using the same factor (1.6) to account for non-C atoms in secondary organic

matter (SOM = 1.6SOC) the total secondary mass (SIA + SOM) is variable from 33% to 43% of PM_{10} and from 46% to 62% of $PM_{2.5}$. These percentages are comparable with those observed in Barcelona (Spain) and lower than those observed in Northern and Central Italy (Amato et al., 2016).

In order to better understand the seasonal variability of SIA, the equivalent concentrations of NH_4^+, SO_4^{2-}, and NO_3^- in $PM_{2.5}$ are reported in Fig. 5. In spring, autumn and summer, ammonium concentrations are lower than what is necessary to completely neutralize sulphate, however, in winter there is an excess of ammonium with respect to sulphate suggesting the possibility of ammonium nitrate formation. Considering also the relatively low chloride depletion (discussed in Section 3.4) in sea-spray observed in winter, it is likely that the two forms of nitrate (sodium and ammonium nitrate) coexist mainly during winter.

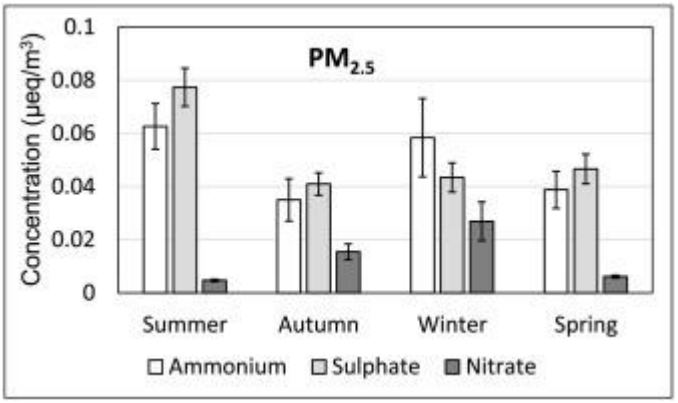

1. Download : Download high-res image (117KB)
2. Download : Download full-size image

Fig. 5

3.4. Sea-spray and crustal sources

The correlations observed between Na^+, Cl^-, and Mg^{2+} indicates that the site is influenced by sea-spray (Querol et al., 2001a). The yearly averages of Cl^-/Na^+ ratios were 0.76 (± 0.06) in PM_{10} and 0.94 (± 0.11) in $PM_{2.5}$, significantly lower than the expected value (1.81) in sea water (Prodi et al., 2009). This indicates that, on average, sea-spray reaching the site is relatively aged as consequence of chemical reactions involving NaCl and nitric acid which lead to the formation of $NaNO_3$ and gaseous HCl (McInnes et al., 1994, Pio et al., 1996, Zhao and Gao, 2008). This explains the chloride depletion and, in turn, the low Cl^-/Na^+ that was observed also in previous studies in the same area (Contini et al., 2014b, Guascito et al., 2015). The yearly average percentages of depleted Cl^- are 60% (± 3%) in both size fractions. The sea spray contribution, evaluated as $Cl^- + 1.4468 * Na^+$ (Marenco et al., 2006), is reported in Table S1. The percentages of depleted Cl^- are comparable in fine and coarse fractions and are maximum during the warm seasons as shown in Fig. 6a. Consequently, the Cl^-/Na^+ ratio is lower during warm seasons with respect to cold seasons. The sea spray contributions to $PM_{2.5}$ and to coarse fraction, for the different seasons, are compared in Fig. 6b. Sea spray ranges from 2.3% to 3.5% in $PM_{2.5}$ and from 12.2% to 19.4% in the coarse fraction. Thereby, as expected, this source influences mainly large particles. The minimum contribution to measured concentrations is observed during summer.

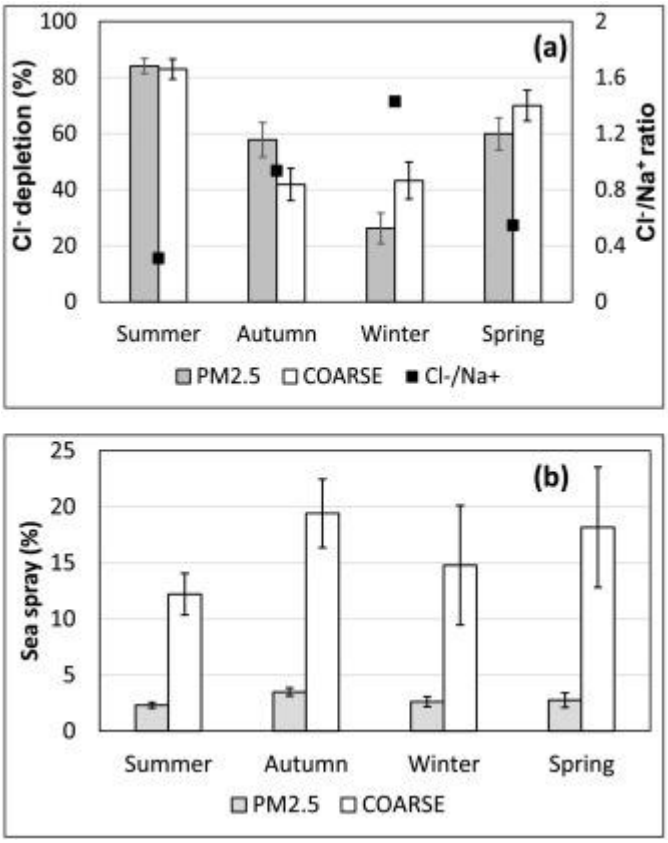

1. Download : Download high-res image (215KB)
2. Download : Download full-size image

Fig. 6

Crustal contribution can be calculated summing the concentration of elements (as metal oxides) generally associated with mineral dust: Al, Si, and Fe plus the insoluble fraction of K and Ca (indicated with an asterisk) as 1.15 (1.89 Al + 2.14 Si + 1.67 Ti + 1.4 Ca* + 1.2 K* + 1.36 Fe) and carbonates calculated from non-sea-salt calcium and magnesium as 1.5 nss-Ca^{2+} + 2.5 nss-Mg^{2+} (Perrino et al., 2014, Cesari et al., 2016c). The factor 1.15 takes into account sodium and magnesium oxides (Marcazzan et al., 2001). The Si concentrations, not measured, were estimated considering that $3Al_2O_3 = SiO_2$ thereby giving Si = 2.65 Al (Querol et al.,

2001b). The typical ratio between water soluble and total concentration of Ca and K, measured in the Apulia (SE Italy) region (Contini et al., 2010) were used. The non-sea-salt component of Ca^{2+} was evaluated as nss-Ca^{2+} = Ca^{2+} – 0.038 Na^{+} and that of Mg^{2+} as nss-Mg^{2+} = Mg^{2+} – 0.129 Na^{+}. The ionic balance indicates a good correlation between total anions and total cations concentrations in PM_{10} (Fig. 7a). However, there was an anion deficit (deficit in negative charges). The same apply for $PM_{2.5}$ (not shown) even if the deficit was lower in relative terms about 7.1% (in terms of charges) in $PM_{2.5}$ compared to 27.7% in PM_{10}. Organic ions, such as formate and acetate, could contribute to the ionic balance; however, the presence of an anion deficit was used, in several sites, to infer the presence and to estimate the concentration of carbonates (CO_3^{2-}/HCO_3^{-}) in aerosols (Nicolás et al., 2009, Arsene et al., 2011, Shen et al., 2011, Contini et al., 2014b). Fig. 7b shows that the observed anion deficit is well correlated with the sum of nss-Ca^{2+} and nss-Mg^{2+}. This suggests the presence of a contribution of calcium and magnesium carbonates due to resuspended local soil that is mainly limestone thereby having relevant Ca content (Cesari et al., 2012).

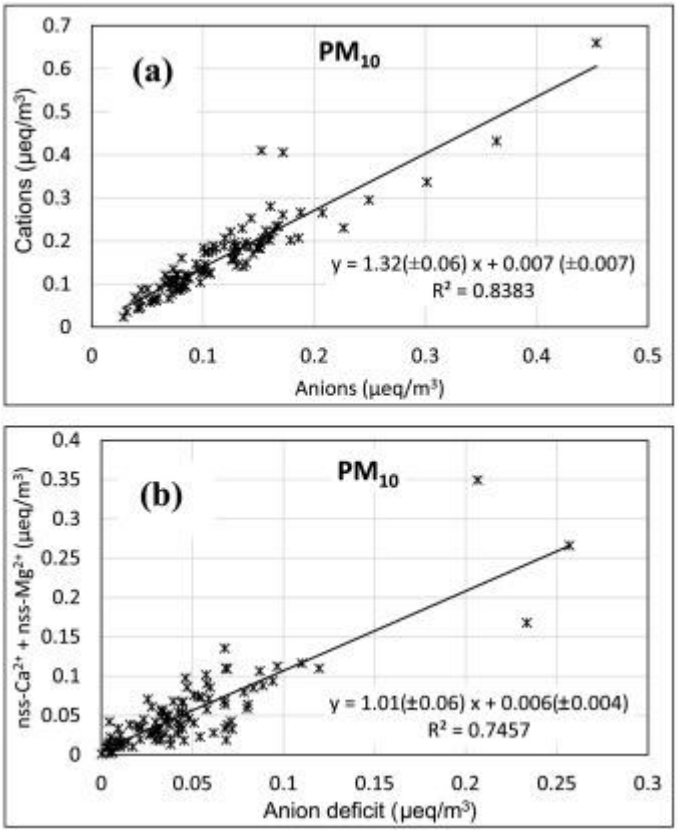

1. Download : Download high-res image (285KB)
2. Download : Download full-size image

Fig. 7

The crustal and carbonates contributions to $PM_{2.5}$ and to the coarse fraction are reported, for the different seasons, in Fig. 8, including the total mineral contribution calculated as the sum of crustal and carbonates contributions. Results show that both crustal and carbonates components have larger concentrations in the coarse particles, however, their contributions to fine particles are not negligible. This was observed also in other studies, for example, crustal and carbonates were observed in $PM_{2.5}$ in several sites (Ho et al., 2011, Arsene et al., 2011, Cesari et al., 2014, Cesari et al., 2016b). Carbonates contributions present a clear seasonal variability

with a decrease in winter and spring on both size fractions. Crustal contributions have similar contributions to $PM_{2.5}$ for the different seasons instead a clear variability is observed in the coarse fraction with contributions in winter and spring lower than those in summer and autumn. This difference among the two size fractions is observed also for the total mineral contribution that is similar during the four seasons for $PM_{2.5}$ but the coarse fraction decreases passing from the warm to the cold seasons. The decrease of total mineral contribution in coarse fraction is correlated with precipitations. The percentages of sampling days with precipitations (> 1 mm H_2O/day) are 6.5% (summer), 17.6% (autumn), 35% (winter), and 39.3% (spring). This suggests that local dust due to resuspension decreases when soil humidity increases and that wet scavenging remove more efficiently coarse particles.

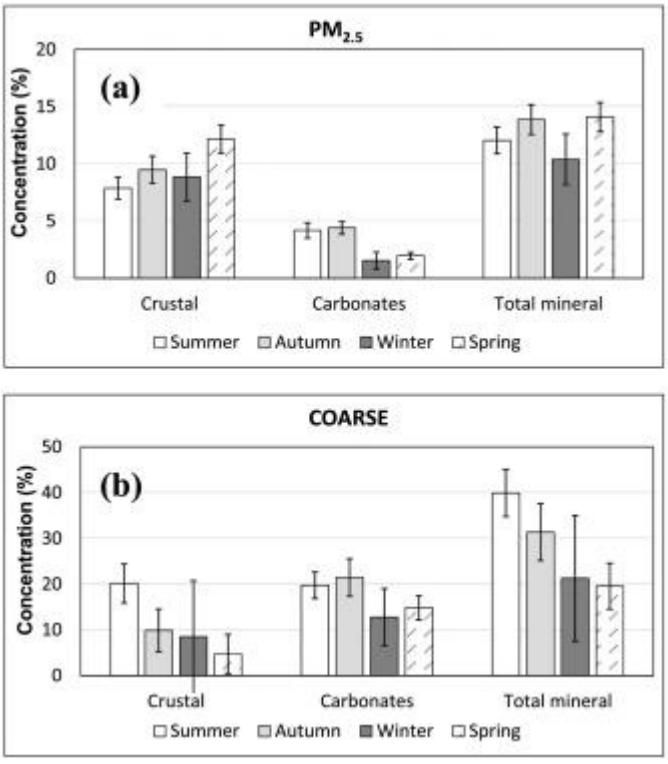

1. Download : Download high-res image (209KB)
2. Download : Download full-size image

Fig. 8

4. Results of PMF5 source apportionment

4.1. Source profiles

The profiles of the different factors, with the corresponding uncertainties, are shown in Fig. S2. The first factor was associated to marine contribution being loaded with Na^+ and Cl^-. The second factor was characterised by K^+ and, to a lower degree by OC and EC suggesting its association with biomass burning and fires (Almeida et al., 2006, Zhang et al., 2008b). The third factor represents likely an industrial contribution characterised mainly by Pb. The fourth factor was loaded with EC, OC, Cu, Zn, Mn, and Sb and it represented the contribution of road traffic. The fifth factor was characterised by Al, Ti, V, Fe, Sr, Nb, La, and Ce that are elements generally associated to crustal minerals as it was confirmed by the analysis of the crustal enrichment factors (Section 3.2). The sixth factor was loaded with Ca^{2+} and Mg^{2+} and it represented resuspended dust contribution. This contribution includes carbonate/bicarbonate (likely calcium and magnesium carbonate), often observed in coarse aerosol, that could originate from local crustal material (Contini et al., 2014b). The presence of carbonates/bicarbonates was also inferred by the analysis of the ionic balance showing an anion deficit (Fig. 7) associated to the CO_3^{2-}/HCO_3^- ions not quantified by ion chromatography. It is interesting to observe that the ability of PMF5 to separate these contributions is likely due to the different dynamics of crustal and carbonates materials. This was observed also in other works in Southern (Cesari et al., 2016b) and Central Italy (Amato et al., 2016, Contini et al., 2016). Crustal material is associated to long-range transport (including advection of Saharan dust) instead carbonates are associated to local resuspension. The seventh and eighth factors represent secondary nitrate and sulphate respectively.

The PMF5 run, applied with the constraints mentioned in Section 2.3, identifies a secondary nitrate component of sodium nitrate due to the interaction of nitric acid with marine aerosol. However, the balance between ammonium, nitrate and sulphate (Fig. 4) suggested the presence of ammonium nitrate during winter at low temperature. As a consequence, nitrate during winter period was underestimated by the PMF5 reconstruction. Therefore, a new PMF5 run was performed with explicit constraints to increase nitrate contribution limited to the winter period. This allowed finding an ammonium nitrate profile shown in Fig. S2. The contribution to measured concentration of both forms of nitrate was calculated from this PMF5 solution.

4.2. Seasonal variabilities of source contributions and their correlation with meteorology

The seasonal variabilities of source contributions to $PM_{2.5}$ and to PM_{10} obtained using PMF5 are reported in Fig. 9. The yearly average contributions for $PM_{2.5}$ and coarse fractions are compared in Fig. 9c. Marine, crustal, and carbonates sources are mainly present in the coarse fraction with seasonal variabilities in reasonable agreement with the behaviours inferred by the mass closure analysis (Section 3.4). Ammonium nitrate and sulphate are larger in $PM_{2.5}$ fraction with respect to the coarse fraction and present an opposite variability with ammonium sulphate reaching maximum concentration in summer and ammonium nitrate in winter. The comparison with mass closure analysis showed that PMF slight overestimated sulphate. Industrial contributions are larger on $PM_{2.5}$ with respect to the coarse fraction and limited to 4–5% of mass concentration. Traffic is an important source in both size fractions with a clear seasonal variability with larger concentrations in autumn and winter, likely because of the increased vehicular traffic at the University Campus during the cold period. Biomass burning is one of the most important source at the site

studied. It is mainly associated to the fine fraction and it has the obvious seasonal variability with larger contributions during autumn and winter, however, its weight is not negligible in spring and summer even if domestic heating are not present. This was observed also in other areas in southern Italy (Cesari et al., 2014) and it is likely due to a contribution from fires and agricultural practices. This is in agreement with Cristofanelli et al. (2017) who reported very high CO values (a “golden” tracer for combustion emissions) during winter 2015 but still high values during spring-summer for this area.

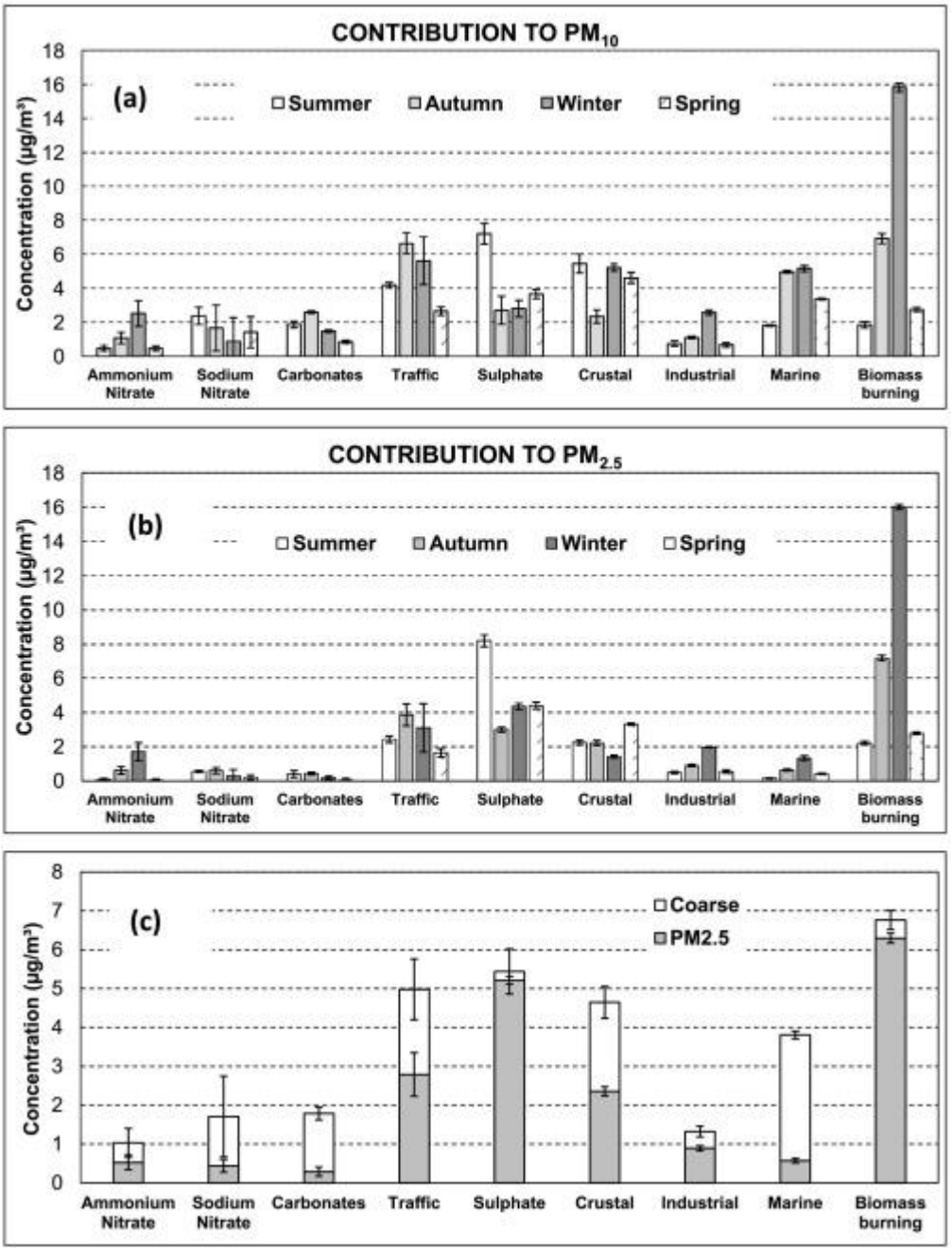

1. Download : Download high-res image (687KB)
2. Download : Download full-size image

Fig. 9

Seasonal variabilities put in evidence a correlation of composition and sources with temperature. To better analyse the correlation with meteorology, an average wind velocity and a prevalent wind direction was calculated for each measurement day. These values were used to produce pollution roses for the different sources dominant in PM_{10} (Fig. S3) and in $PM_{2.5}$ (Fig. S4). In Figs. S3 and S4 the average contribution of each source is reported as a colour scale, the distance from the centre is proportional to the wind velocity and the angular position represents the wind direction. Fig. S3 shows that larger crustal contributions are associated to relatively high wind velocities from SE direction, similar to the pattern observed for marine contributions. Instead, carbonates are mainly associated to high wind velocity from the North direction. This difference in the dynamics of carbonates and crustal dust is likely one of the reason that allowed a clear separation of these sources in PMF results. Fig. S4 shows a pollution rose for $PM_{2.5}$ different from that of PM_{10} because large $PM_{2.5}$ concentrations do not have a specific directionality and happens at low wind velocity. A similar pattern is observed also for biomass burning, traffic and ammonium nitrate contributions. Instead, sulphate and industrial contributions have a different pattern with larger values associated to high winds from North. The similarity of the sulphate and industrial pollution roses suggests that secondary sulphate originates at larger distances from the site where industrial emissions of SO_2 are present and could be partly converted in sulphate.

A back-trajectories analysis has been performed in order to infer potential locations of distant sources using Concentration Weighted Trajectory (CWT) analysis (Stohl, 1998, Hsu et al., 2003, Squizzato and Masiol, 2015). Here, the CWT approach (Seibert et al., 1994, Hsu et al., 2003) was chosen since it is suitable to quantify long-range transported aerosol (Jeong et al., 2011). Details of the method used and CWT results are summarized in Supplementary material. Back-trajectories were computed by the Hybrid

Single-Particle Lagrangian Integrated Trajectory (HYSPLIT4) model (Stein et al., 2015, Rolph, 2016) using the Global NOAA-NCEP/NCAR Reanalysis meteorological data. The HYSPLIT parameters were set as: total run time 72 h, start time at midnight, starting height of 100 m above ground level (agl) at the measurement site. This height allowed an effective transport within the mixing layer, as suggested elsewhere (Begum et al., 2005, Jeong et al., 2011, Westgate and Wania, 2011). Calculations were also performed starting at 50 m (agl) and no significant differences were observed (not shown). Assuming that the use of multiple trajectory–based models over long period may yield more robust results than using individual trajectories (Squizzato and Masiol, 2015), multiple back-trajectories were simulated starting every 3 h.

In Fig. S5 CWT results for biomass burning, industrial, ammonium nitrate, sulphate and traffic contributions are shown for the $PM_{2.5}$ fraction. The analysis shows for biomass burning probable source areas over the countries of Albania, Macedonia and North of Greece. This evidence confirms previous investigations carried out in Greece (Saffari et al., 2013) indicating a growing impact of biomass burning due to the switch from heating oil to cheaper material, such as wood, as burning material in residential heating for economic crisis. Industrial and secondary ammonium nitrate contributions present similar source areas (mainly over central and northern Italy) indicating a probable common origin. Conversely, the secondary sulphate seems to be associated to a more extended source area, reflecting different effects due to multiple sources i.e. industrial and/or ship traffic in the Adriatic Sea (Merico et al., 2017) or the effect of different meteorological conditions. Finally, it is quite interesting to note that traffic source does not show a long-range source area, highlighting the local nature of this source.

In Fig. S6 CWT results for carbonate, crustal, marine and sodium nitrate are shown for the PM_{10} fraction. The analysis showed a main local source area for carbonate and crustal contributions also highlighting the presence of a source area in North Africa, confirming that the Mediterranean area is influenced by crustal matter long-range transport events. As expected, the source area of the marine contribution is represented by the Ionian and Libyan Sea. More interesting is the area reported for sodium nitrate, indicating the contribution coming from both the sea and lands of south Italy and south Est Europe. This is probably due to interaction between fresh sea spray and polluted air with consequent formation of aged sea salt (sodium nitrate).

5. Conclusions

An analysis of seasonal variabilities of fine ($PM_{2.5}$) and coarse ($PM_{2.5–10}$) particulate matter concentrations and composition was performed at an urban background station in Southern Italy. The seasonal variability of the contributions of nine sources (marine, sulphate, sodium nitrate, ammonium nitrate, biomass burning, traffic, industrial, crustal, and carbonates) was investigated using both mass closure and PMF5 receptor models.

Results show that marine contributions, dominant in the coarse fraction, are mainly associated with high winds from SE direction and they are larger during the cold period (autumn and winter) with respect to the warm period (spring and summer). Chloride depletion is relevant in both size fractions with a clear seasonal variability reaching a minimum of 26% (in $PM_{2.5}$) and 43% (in $PM_{2.5–10}$) during winter. This depletion is correlated with the formation of sodium nitrate in the coarse fraction.

Organic and inorganic secondary aerosol accounts for 43% of $PM_{2.5}$ and 12% of $PM_{2.5–10}$ with small seasonal changes. However, seasonal pattern of

SIA is opposite to that of SOC. SOC is larger during the cold period and sulphate (the major contributor to SIA) is larger during summer. Two forms of nitrate were identified: sodium and ammonium nitrate. $NaNO_3$ is mainly present in the coarse fraction during spring, autumn and summer while NH_4NO_3 is present only during winter and it is more abundant in the fine fraction like sulphate.

Mass closure analysis and PMF results identify two soil sources: crustal associated mainly to long range transport and carbonates associated to local resuspended dust. Both sources contributes mainly to the coarse fraction and have different dynamics with crustal source contributing mainly in high winds from SE conditions and carbonates during high winds from North direction. Total mineral contribution does not present a seasonal variability in $PM_{2.5}$ but, in the coarse fraction, it decreases during the cold seasons, likely because of the scavenging effect of precipitations.

Biomass burning is a relevant source for this area with larger contribution during autumn and winter because of the influence of domestic heating, however, this source is not negligible in spring and summer, likely because of the contributions of fires and agricultural practices.

Industrial contribution is mainly in $PM_{2.5}$ contributing for about 4–5% of $PM_{2.5}$ and it is correlated with wind velocities and directions similarly to secondary sulphate suggesting a common origin.

Traffic is a source contributing to both size fractions ($PM_{2.5}$ and $PM_{2.5–10}$). Its weight on PM mass concentrations increases during autumn and winter. Traffic contribution has not a specific directionality and it is larger at low wind velocities with limited ventilation.

Acknowledgements

This work was funded by I-AMICA (Infrastructure of High Technology for Environmental and Climate Monitoring - PONa3_00363), a project of structural improvement financed under the National Operational Program (NOP) for “Research and Competitiveness 2007–2013” co-funded with European Regional Development Fund (ERDF) and National resources.

Appendix A. Supplementary data

Download : **Download Word document (3MB)**

Supplementary material

References

Aldabe et al., 2013

J. Aldabe, C. Santamaría, D. Elustondo, E. Lasheras, J.M. Santamaría

Application of microwave digestion and ICP-MS to simultaneous analysis of major and trace elements in aerosol samples collected on quartz filters

Anal. Methods, 5 (2013), pp. 554-559

View Record in ScopusGoogle Scholar

Almeida et al., 2006

S.M. Almeida, C.A. Pio, M.C. Freitas, M.A. Reis, M.A. Trancoso

Approaching PM2.5 and PM2.5–10 source apportionment by mass balance analysis, principal component analysis and particle size distribution

Sci. Total Environ., 368 (2006), pp. 663-674

ArticleDownload PDFView Record in ScopusGoogle Scholar

Amato et al., 2009

F. Amato, M. Pandolfi, A. Escrig, X. Querol, A. Alastuey, J. Pey, N. Pérez, P.K. Hopke

Quantifying road dust resuspension in urban environment by multilinear engine: a comparison with PMF2

Atmos. Environ., 43 (2009), pp. 2770-2780

ArticleDownload PDFView Record in ScopusGoogle Scholar

Amato et al., 2014

F. Amato, A. Karanasiou, P. Cordoba, A. Alastuey, T. Moreno, F. Lucarelli, S. Nava, G. Calzolai, X. Querol

Effects of road dust suppressants on PM levels in a Mediterranean urban area

Environ. Sci. Technol., 48 (2014), pp. 8069-8077

View PDFCrossRefView Record in ScopusGoogle Scholar

Amato et al., 2016

F. Amato, A. Alastuey, A. Karanasiou, F. Lucarelli, S. Nava, G. Calzolai, M. Severi, S. Becagli, L.G. Vorne, C. Colombi, C. Alves, D. Custódio, T. Nunes, M. Cerqueira, C. Pio, K. Eleftheriadis, E. Diapouli, C. Reche, M.C. Minguillón, M.I. Manousakas, T. Maggos, S. Vratolis, R.M. Harrison, X. Querol

AIRUSE-LIFEC: a harmonized PM speciation and source apportionment in five southern European cities

Atmos. Chem. Phys., 16 (2016), pp. 3289-3309

View PDFCrossRefView Record in ScopusGoogle Scholar

Andreae and Merlet, 2001

M.O. Andreae, P. Merlet

Emission of trace gases and aerosols from biomass burning

Glob. Biogeochem. Cycles, 15 (2001), pp. 955-966

View Record in ScopusGoogle Scholar

Arsene et al., 2011

C. Arsene, R.I. Olariu, P. Zarmpas, M. Kanakidou, N. Mihalopoulos

Ion composition of coarse and fine particles in Iasi, north-eastern Romania: implications for aerosol chemistry in the area

Atmos. Environ., 45 (2011), pp. 906-916

ArticleDownload PDFView Record in ScopusGoogle Scholar

Artíñano et al., 2001

B. Artíñano, X. Querol, P. Salvador, S. Rodríguez, D.G. Alonso, A. Alastuey

Assessment of airborne particulate levels in Spain in relation to the new EU-directive

Atmos. Environ., 35 (Supplement 1) (2001), pp. S43-S53

ArticleDownload PDFView Record in ScopusGoogle Scholar

Begum et al., 2005

B.A. Begum, E. Kim, C.H. Jeong, D.W. Lee, P.K. Hopke

Evaluation of the potential source contribution function using the 2002 Quebec forest fire episode

Atmos. Environ., 39 (2005), pp. 3719-3724

View Record in ScopusGoogle Scholar

Belis et al., 2013

C.A. Belis, F. Karagulian, B.R. Larsen, P.K. Hopke

Critical review and meta-analysis of ambient particulate matter source apportionment using receptor models in Europe

Atmos. Environ., 69 (2013), pp. 94-108

ArticleDownload PDFView Record in ScopusGoogle Scholar

Blanchard et al., 2016

C.L. Blanchard, G.M. Hidy, S. Shaw, K. Baumann, E.S. Edgerton

Effects of emission reductions on organic aerosol in the southeastern United States

Atmos. Chem. Phys., 16 (2016), pp. 215-238

View PDFCrossRefView Record in ScopusGoogle Scholar

Brunekreef and Forsberg, 2005

B. Brunekreef, B. Forsberg

Epidemiological evidence of effects of coarse airborne particles on health

Eur. Respir. J., 26 (2005), pp. 309-318

View PDFCrossRefView Record in ScopusGoogle Scholar

Cesari et al., 2012

D. Cesari, D. Contini, A. Genga, M. Siciliano, C. Elefante, F. Baglivi, L. Daniele

Analysis of raw soils and their re-suspended PM10 fractions: characterisation of source profiles and enrichment factors

Appl. Geochem., 27 (2012), pp. 1238-1246

ArticleDownload PDFView Record in ScopusGoogle Scholar

Cesari et al., 2014

D. Cesari, A. Genga, P. Ielpo, M. Siciliano, G. Mascolo, F.M. Grasso, D. Contini

Source apportionment of PM2.5 in the harbour–industrial area of Brindisi (Italy): identification and estimation of the contribution of in-port ship emissions

Sci. Total Environ., 497–498 (2014), pp. 392-400

ArticleDownload PDFView Record in ScopusGoogle Scholar

Cesari et al., 2016a

D. Cesari, A. Donateo, M. Conte, D. Contini

Inter-comparison of source apportionment of PM10 using PMF and CMB in three sites nearby an industrial area in central Italy

Atmos. Res., 182 (2016), pp. 282-293

ArticleDownload PDFView Record in ScopusGoogle Scholar

Cesari et al., 2016b

D. Cesari, A. Donateo, M. Conte, E. Merico, A. Giangreco, F. Giangreco, D. Contini

An inter-comparison of PM2.5 at urban and urban background sites: chemical characterization and source apportionment

Atmos. Res., 174–175 (2016), pp. 106-119

ArticleDownload PDFView Record in ScopusGoogle Scholar

Cesari et al., 2016c

D. Cesari, F. Amato, M. Pandolfi, A. Alastuey, X. Querol, D. Contini

An inter-comparison of PM10 source apportionment using PCA and PMF receptor models in three European sites

Environ. Sci. Pollut. Res., 23 (15) (2016), pp. 15133-15148

View PDFCrossRefView Record in ScopusGoogle Scholar

Chirizzi et al., 2017

D. Chirizzi, D. Cesari, M.R. Guascito, A. Dinoi, L. Giotta, A. Donateo, D. Contini

Influence of Saharan dust outbreaks and carbon content on oxidative potential of water-soluble fractions of PM2.5 and PM10

Atmos. Environ., 163 (2017), pp. 1-8

ArticleDownload PDFView Record in ScopusGoogle Scholar

Contini et al., 2010

D. Contini, A. Genga, D. Cesari, M. Siciliano, A. Donateo, M.C. Bove, M.R. Guascito

Characterization and source apportionment of PM10 in an urban background site in Lecce

Atmos. Res., 95 (2010), pp. 40-54

ArticleDownload PDFView Record in ScopusGoogle Scholar

Contini et al., 2012

D. Contini, F. Belosi, A. Gambaro, D. Cesari, A.M. Stortini, M.C. Bove

Comparison of PM_{10} concentrations and metal content in three different sites of the Venice Lagoon: an analysis of possible aerosol sources

J. Environ. Sci., 24 (2012), pp. 1954-1965

ArticleDownload PDFView Record in ScopusGoogle Scholar

Contini et al., 2014a

D. Contini, D. Cesari, A. Donateo, D. Chirizzi, F. Belosi

Characterization of PM_{10} and $PM_{2.5}$ and their metals content in different typologies of sites in South-Eastern Italy

Atmos., 5 (2014), pp. 435-453

View PDFCrossRefView Record in ScopusGoogle Scholar

Contini et al., 2014b

D. Contini, D. Cesari, A. Genga, M. Siciliano, P. Ielpo, M.R. Guascito, M. Conte

Source apportionment of size-segregated atmospheric particles based on the major water-soluble components in Lecce (Italy)

Sci. Total Environ., 472 (2014), pp. 248-261

ArticleDownload PDFView Record in ScopusGoogle Scholar

Contini et al., 2016

D. Contini, D. Cesari, M. Conte, A. Donateo

Application of PMF and CMB receptor models for the evaluation of the contribution of a large coal-fired power plant to PM10 concentrations

Sci. Total Environ., 560–561 (2016), pp. 131-140

ArticleDownload PDFView Record in ScopusGoogle Scholar

Cristofanelli et al., 2016

P. Cristofanelli, T.C. Landi, F. Calzolari, R. Duchi, A. Marinoni, M. Rinaldi, P. Bonasoni

Summer atmospheric composition over the Mediterranean basin: investigation on transport processes and pollutant export to the free troposphere by observations at the WMO/GAW Mt. Cimone global station (Italy, 2165 m a.s.l.)

Atmos. Environ., 141 (2016), pp. 139-152

ArticleDownload PDFView Record in ScopusGoogle Scholar

Cristofanelli et al., 2017

P. Cristofanelli, M. Busetto, F. Calzolari, I. Ammoscato, D. Gullì, A. Dinoi, C.R. Calidonna, D. Contini, D. Sferlazzo, T. Di Iorio, S. Piacentino, A. Marinoni, M. Maione, P. Bonasoni

Investigation of reactive gases and methane variability in the coastal boundary layer of the central Mediterranean basin

Elem. Sci. Anth., 5 (2017), p. 12, 10.1525/elementa.216

View PDFView Record in ScopusGoogle Scholar

Delfino et al., 2005

R.J. Delfino, C. Sioutas, S. Malik

Potential role of ultrafine particles in associations between airborne particle mass and cardiovascular health

Environ. Health Perspect., 113 (8) (2005), pp. 934-946

View PDFCrossRefView Record in ScopusGoogle Scholar

Dinoi et al., 2017

A. Dinoi, A. Donateo, F. Belosi, M. Conte, D. Contini

Comparison of atmospheric particle concentration measurements using different optical detectors: potentiality and limits for air quality applications

Measurement, 106 (2017), pp. 274-282

ArticleDownload PDFView Record in ScopusGoogle Scholar

Dockery and Stone, 2007

D.W. Dockery, P.H. Stone

Cardiovascular risks from fine particulate air pollution

N. Engl. J. Med., 356 (2007), pp. 511-513

View PDFCrossRefView Record in ScopusGoogle Scholar

Escudero et al., 2015

M. Escudero, M. Viana, X. Querol, A. Alastuey, Hernández P. Díez, S. García Dos Santos, J. Anzano

Industrial sources of primary and secondary organic aerosols in two urban environments in Spain

Environ. Sci. Pollut. Res., 22 (2015), pp. 10413-10424

Fuzzi et al., 2015

S. Fuzzi, U. Baltensperger, K. Carslaw, S. Decesari, H. Denier van der Gon, M.C. Facchini, D. Fowler, I. Koren, B. Langford, U. Lohmann, E. Nemitz, S. Pandis, I. Riipinen, Y. Rudich, M. Schaap, J.G. Slowik, D.V. Spracklen, E. Vignati, M. Wild, M. Williams, S. Gilardoni

Particulate matter, air quality and climate: lessons learned and future needs

Atmos. Chem. Phys., 15 (2015), pp. 8217-8299

Gauderman et al., 2015

W.J. Gauderman, R. Urman, E. Avol, K. Berhane, R. McConnell, E. Rappaport, R. Chang, F. Lurmann, F. Gilliland

Association of improved air quality with lung development in children

N. Engl. J. Med., 372 (2015), pp. 905-913

Gentner et al., 2012

D.R. Gentner, G. Isaacman, D.R. Worton, A.W.H. Chan, T.R. Dallmann, L. Davis, S. Liu, D.A. Day, L.M. Russell, K.R. Wilson, R. Weber, A. Guha, R.A. Harley, A.H. Goldstein

Elucidating secondary organic aerosol from diesel and gasoline vehicles through detailed characterization of organic carbon emissions

Proc. Natl. Acad. Sci. U. S. A., 109 (2012), pp. 18318-18323

View PDFCrossRefView Record in ScopusGoogle Scholar

Gregoris et al., 2016

E. Gregoris, E. Barbaro, E. Morabito, G. Toscano, A. Donateo, D. Cesari, D. Contini, A. Gambaro

Impact of maritime traffic on polycyclic aromatic hydrocarbons, metals and particulate matter in Venice air

Environ. Sci. Pollut. Res., 23 (2016), pp. 6951-6959

View PDFCrossRefView Record in ScopusGoogle Scholar

Guascito et al., 2015

M.R. Guascito, D. Cesari, D. Chirizzi, A. Genga, D. Contini

XPS surface chemical characterization of atmospheric particles of different sizes

Atmos. Environ., 116 (2015), pp. 146-154

ArticleDownload PDFView Record in ScopusGoogle Scholar

Hildebrandt et al., 2011

L. Hildebrandt, E. Kostenidou, V.A. Lanz, A.S.H. Prevo, U. Baltensperger, N. Mihalopoulos, A. Laaksonen, N.M. Donahue, S.N. Pandis

Sources and atmospheric processing of organic aerosol in the Mediterranean: insights from aerosol mass spectrometer factor analysis

Atmos. Chem. Phys., 11 (2011), pp. 12499-12515

View PDFCrossRefView Record in ScopusGoogle Scholar

Ho et al., 2011

K.F. Ho, R.J. Zhang, S.C. Lee, S.S.H. Ho, S.X. Liu, K. Fung, J.J. Cao, Z.X. Shen, H.M. Xu

Characteristics of carbonate carbon in $PM_{2.5}$ in a typical semi-arid area of Northeastern China

Atmos. Environ., 45 (2011), pp. 1268-1274

ArticleDownload PDFView Record in ScopusGoogle Scholar

Hsu et al., 2003

Y. Hsu, T.M. Holsen, P.K. Hopke

Comparison of hybrid receptor models to locate PCB sources in Chicago

Atmos. Environ., 37 (2003), pp. 545-562

ArticleDownload PDFView Record in ScopusGoogle Scholar

Hsu et al., 2016

C.Y. Hsu, H.C. Chiang, S.L. Lin, M.J. Chena, T.Y. Lina, Y.C. Chena

Elemental characterization and source apportionment of PM10 and PM2.5 in the western coastal area of central Taiwan

Sci. Total Environ., 541 (2016), pp. 1139-1150

ArticleDownload PDFView Record in ScopusGoogle Scholar

Jain et al., 2017

S. Jain, S.K. Sharma, N. Choudhary, R. Masiwal, M. Saxena, A. Sharma, T.K. Mandal, A. Gupta, N.C. Gupta, C. Sharma

Chemical characteristics and source apportionment of PM2.5 using PCA/APCS, UNMIX, and PMF at an urban site of Delhi, India

Environ. Sci. Pollut. Res. Int., 24 (17) (2017), pp. 14637-14656

View PDFCrossRefView Record in ScopusGoogle Scholar

Jeong et al., 2011

U. Jeong, J. Kim, H. Lee, J. Jung, Y.J. Kim, C.H. Song, J.H. Koo

Estimation of the contributions of long range transported aerosol in East Asia to carbonaceous aerosol and PM concentrations in Seoul, Korea using highly time resolved measurements: a PSCF model approach

J. Environ. Monit., 13 (2011), pp. 1905-1918

View PDFCrossRefView Record in ScopusGoogle Scholar

Jerret, 2015

M. Jerret

Atmospheric science: the death toll from air-pollution sources

Nature, 525 (2015), pp. 330-331

Google Scholar

Kamber et al., 2004

B. Kamber, A. Greig, K.A. Collerson

A new estimate for the composition of weathered young upper continental crust from alluvial sediments, Queensland, Australia

Geochim. Cosmochim. Acta, 69 (2004), pp. 1041-1058

Google Scholar

Landis et al., 2017

M.S. Landis, J.P. Pancras, J.R. Graney, E.M. White, E.S. Edgerton, A. Legge, K.E. Percy

Source apportionment of ambient fine and coarse particulate matter at the Fort McKay community site, in the Athabasca Oil Sands Region, Alberta, Canada

Sci. Total Environ., 584–585 (2017), pp. 105-117

ArticleDownload PDFView Record in ScopusGoogle Scholar

Ledoux et al., 2017

F. Ledoux, A. Kfoury, G. Delmaire, G. Roussel, A. El Zein, D. Courcot

Contributions of local and regional anthropogenic sources of metals in PM2.5 at an urban site in northern France

Chemosphere, 181 (2017), pp. 713-724

ArticleDownload PDFView Record in ScopusGoogle Scholar

Lelieveld et al., 2002

J. Lelieveld, H. Berresheim, S. Borrmann, P.J. Crutzen, F.J. Dentener, H. Fischer, J. Feichter, P.J. Flatau, J. Heland, R. Holzinger, R. Korrmann, M.G. Lawrence, Z. Levin, K.M. Markowicz, N. Mihalopoulos, A. Minikin, V. Ramanathan, M. de Reus, G.J. Roelofs, H.A. Scheeren, J. Sciare, H. Schlager, M. Schultz, P. Siegmund, B. Steil, E.G. Stephanou, P. Stier, M. Traub, C. Warneke, J. Williams, H. Ziereis

Global air pollution crossroads over the Mediterranean

Science, 298 (2002), pp. 794-799

View Record in ScopusGoogle Scholar

Lelieveld et al., 2015

J. Lelieveld, J.S. Evans, M. Fnais, D. Giannadaki, A. Pozzer

The contribution of outdoor air pollution sources to premature mortality on a global scale

Nature, 525 (2015), pp. 367-371

View PDFCrossRefGoogle Scholar

Marcazzan et al., 2001

G.M. Marcazzan, S. Vaccaro, G. Valli, R. Vecchi

Characterisation of PM_{10} and $PM_{2.5}$ particulate matter in the ambient air of Milan (Italy)

Atmos. Environ., 35 (2001), pp. 4639-4650

ArticleDownload PDFView Record in ScopusGoogle Scholar

Marenco et al., 2006

F. Marenco, P. Bonasoni, F. Calzolari, M. Ceriani, M. Chiari, P. Cristofanelli, A. D'Alessandro, P. Fermo, F. Lucarelli, F. Mazzei, S. Nava, A. Piazzalunga, P. Prati, G. Valli, R. Vecchi

Characterization of atmospheric aerosols at Monte Cimone, Italy, during summer 2004: source apportionment and transport mechanism

J. Geophys. Res., 111 (2006), Article D24202

View Record in ScopusGoogle Scholar

McInnes et al., 1994

L.M. McInnes, D.S. Covert, P.K. Quinn, M.S. Germani

Measurements of chloride depletion and sulphur enrichment in individual sea-salt particles collected from the remote marine boundary layer

J. Geophys. Res., 99 (1994), pp. 8257-8268

View Record in ScopusGoogle Scholar

Merico et al., 2017

E. Merico, A. Gambaro, A. Argiriou, A. Alebic-Juretic, E. Barbaro, D. Cesari, L. Chasapidis, S. Dimopoulos, A. Dinoi, A. Donateo, C. Giannaros, E. Gregoris, A. Karagiannidis, A.G. Konstandopoulos, T. Ivoševic, N. Liora, D. Melas, B. Mifka, I. Orlic, A. Poupkou, K. Sarovic, A. Tsakis, R. Giua, T. Pastore, A. Nocioni, D. Contini

Atmospheric impact of ship traffic in four Adriatic-Ionian port-cities: comparison and harmonization of different approaches

Transp. Res. Part D: Transp. Environ., 50 (2017), pp. 431-445

ArticleDownload PDFView Record in ScopusGoogle Scholar

Nicolás et al., 2009

J.F. Nicolás, N. Galindo, E. Yubero, C. Pastor, R. Esclapez, J. Crespo

Aerosol inorganic ions in a semiarid region on the Southeastern Spanish Mediterranean coast

Water Air Soil Pollut., 201 (2009), pp. 149-159

View PDFCrossRefView Record in ScopusGoogle Scholar

Paatero and Hopke, 2003

P. Paatero, P.K. Hopke

Discarding or down weighting high-noise variables in factor analytic models

Anal. Chim. Acta, 490 (2003), pp. 277-289

ArticleDownload PDFView Record in ScopusGoogle Scholar

Paatero and Tapper, 1994

P. Paatero, U. Tapper

Positive matrix factorization - a nonnegative factor model with optimal utilization of error-estimates of data values

Environmetrics, 5 (2) (1994), pp. 111-126

View PDFCrossRefView Record in ScopusGoogle Scholar

Paatero et al., 2014

P. Paatero, S. Eberly, S.G. Brown, G.A. Norris

Methods for estimating uncertainty in factor analytic solutions

Atmos. Meas. Tech., 7 (3) (2014), pp. 781-797

View PDFCrossRefView Record in ScopusGoogle Scholar

Pakbin et al., 2011

P. Pakbin, Z. Ning, M.M. Shafer, J.J. Schauer, C. Sioutas

Seasonal and spatial coarse particle elemental concentrations in the Los Angeles area

Aerosol Sci. Technol., 45 (2011), pp. 949-963

View PDFCrossRefView Record in ScopusGoogle Scholar

Pandolfi et al., 2011

M. Pandolfi, Y. Gonzalez-Castanedo, A. Alastuey, J.D. de la Rosa, E. Mantilla, A. Sanchez de la Campa, X. Querol, J. Pey, F. Amato, T. Moreno

Source apportionment of PM10 and PM2.5 at multiple sites in the strait of Gibraltar by PMF: impact of shipping emissions

Environ. Sci. Pollut. Res., 28 (2011), pp. 260-269

Perrino et al., 2014

C. Perrino, M. Catrambone, Torre S. Dalla, E. Rantica, T. Sargolini, S. Canepari

Seasonal variations in the chemical composition of particulate matter: a case study in the Po Valley. Part I: macro-components and mass closure

Environ. Sci. Pollut. Res., 21 (2014), pp. 3999-4009

Pey et al., 2009

J. Pey, N. Pérez, S. Castillo, M. Viana, T. Moreno, M. Pandolfi, J.M. López-Sebastián, A. Alastuey, X. Querol

Geochemistry of regional background aerosols in the Western Mediterranean

Atmos. Res., 94 (2009), pp. 422-435

Pio et al., 1996

C.A. Pio, L.M. Castro, M.A. Cerqueira, I.M. Santos, F. Belchior, M.L. Salgueiro

Source assessment of particulate air pollutants measured at the southwest European coast

Atmos. Environ., 19 (1996), pp. 3309-3320

ArticleDownload PDFView Record in ScopusGoogle Scholar

Pio et al., 2011

C. Pio, M. Cerqueira, R.M. Harrison, T. Nunes, F. Mirante, C. Alves, C. Oliveira, A. Sanchez de la Campa, B. Artíñano, M. Matos

OC/EC ratio observations in Europe: re-thinking the approach for apportionment between primary and secondary organic carbon

Atmos. Environ., 45 (2011), pp. 6121-6132

ArticleDownload PDFView Record in ScopusGoogle Scholar

Pope et al., 2004

C.A. Pope, R.T. Burnett, G.D. Thurston, M.J. Thun, E.E. Calle, D. Krewski, J.J. Godleski

Cardiovascular mortality and long-term exposure to particulate air pollution epidemiological evidence of general pathophysiological pathways of disease

Circulation, 109 (2004), pp. 71-77

Prodi et al., 2009

F. Prodi, F. Belosi, D. Contini, G. Santachiara, L. Di Matteo, A. Gambaro, A. Donateo, D. Cesari

Aerosol fine fraction in the Venice lagoon: particle composition and sources

Atmos. Res., 92 (2009), pp. 141-150

ArticleDownload PDFView Record in ScopusGoogle Scholar

Pulong et al., 2017

C. Pulong, W. Tijian, D. Mei, M. Kasoar, H. Yong, X. Min, L. Shu, Z. Bingliang, L. Mengmeng, H. Tunan

Characterization of major natural and anthropogenic source profiles for size-fractionated PM in Yangtze River Delta

Sci. Total Environ., 598 (2017), pp. 135-145

Google Scholar

Querol et al., 2001a

X. Querol, A. Alastuey, S. Rodriguez, F. Plana, E. Mantilla, C.R. Ruiz

Monitoring of PM10 and PM2.5 around primary particulate anthropogenic emission sources

Atmos. Environ., 35 (2001), pp. 845-858

ArticleDownload PDFView Record in ScopusGoogle Scholar

Querol et al., 2001b

X. Querol, A. Alastuey, S. Rodriguez, F. Plana, C.R. Ruiz, N. Cots, G. Massague, O. Puig

PM10 and PM2.5 source apportionment in the Barcelona Metropolitan area, Catalonia, Spain

Atmos. Environ., 35 (2001), pp. 6407-6419

ArticleDownload PDFGoogle Scholar

Querol et al., 2008

X. Querol, A. Alastuey, T. Moreno, M.M. Viana, S. Castillo, J. Pey, S. Rodríguez, B. Artiñano, P. Salvador, M. Sánchez, S. Garcia Dos Santos, M.D. Herce Garraleta, R. Fernandez-Patier, S. Moreno-Grau, L. Negral, M.C. Minguillón, E. Monfort, M.J. Sanz, R. Palomo-Marín, E. Pinilla-Gil, E. Cuevas, J. de la Rosa, A. Sánchez de la Campa

Spatial and temporal variations in airborne particulate matter (PM10 and PM2.5) across Spain 1999–2005

Atmos. Environ., 42 (2008), pp. 3964-3979

ArticleDownload PDFView Record in ScopusGoogle Scholar

Ripoll et al., 2015

A. Ripoll, M.C. Minguillón, J. Pey, N. Pérez, X. Querol, A. Alastuey

Joint analysis of continental and regional background environments in the western Mediterranean: PM1 and PM10 concentrations and composition

Atmos. Chem. Phys., 15 (2015), pp. 1129-1145

View PDFCrossRefView Record in ScopusGoogle Scholar

Robinson et al., 2007

A.L. Robinson, N.M. Donahue, M.K. Shrivastava, E.A. Weitkamp, A.M. Sage, A.P. Grieshop, T.E. Lane, J.R. Pierce, S.N. Pandis

Rethinking organic aerosols: semivolatile emissions and photochemical aging

Science, 315 (2007), pp. 1259-1262

View PDFCrossRefView Record in ScopusGoogle Scholar

Rolph, 2016

G.D. Rolph

Real-time environmental applications and display system (READY)

Website

NOAA Air Resources Laboratory, College Park, MD, http://www.ready.noaa.gov (2016)

Google Scholar

Saffari et al., 2013

A. Saffari, N. Daher, C. Samara, D. Voutsa, A. Kouras, E. Manoli, O. Karagkiozidou, C. Vlachokostas, N. Moussiopoulos, M.M. Shafer, J.J. Schauer, C. Sioutas

Increased biomass burning due to the economic crisis in Greece and its adverse impact on wintertime air quality in Thessaloniki

Environ. Sci. Technol., 47 (2013), pp. 13313-13320

View PDFCrossRefView Record in ScopusGoogle Scholar

Sahu et al., 2011

L.K. Sahu, Y. Kondo, Y. Miyazaki, P. Pongkiatkul, N.T.K. Oanh

Seasonal and diurnal variations of black carbon and organic carbon aerosols in Bangkok

J. Geophys. Res., 116 (2011), Article D15302

View Record in ScopusGoogle Scholar

Salameh et al., 2015

D. Salameh, A. Detournay, J. Pey, N. Pérez, F. Liguori, D. Saraga, M.C. Bove, P. Brotto, F. Cassola, D. Massabò, A. Latella, S. Pillon, G. Formenton, S. Patti, A. Armengaud, D. Piga, J.L. Jaffrezo, J. Bartzis, E. Tolis, P. Prati, X. Querol, H. Wortham, N. Marchand

PM2.5 chemical composition in five European Mediterranean cities: a 1-year study

Atmos. Res., 155 (2015), pp. 102-117

ArticleDownload PDFView Record in ScopusGoogle Scholar

Sandrini et al., 2014

S. Sandrini, S. Fuzzi, A. Piazzalunga, P. Prati, P. Bonasoni, F. Cavalli, M.C. Bove, M. Calvello, D. Cappelletti, C. Colombi, D. Contini, G. de Gennaro, A. Di Gilio, P. Fermo, L. Ferrero, V. Gianelle, M. Giugliano, P. Ielpo, G. Lonati, A. Marinoni, D. Massabò, U. Molteni, B. Moroni, G. Pavese, C. Perrino, M.G. Perrone, M.R. Perrone, J.P. Putaud, T. Sargolini, R. Vecchi, S. Gilardoni

Spatial and seasonal variability of carbonaceous aerosol across Italy

Atmos. Environ., 99 (2014), pp. 587-598

ArticleDownload PDFView Record in ScopusGoogle Scholar

Seibert et al., 1994

P. Seibert, H. Kromp-Kolb, U. Baltensperger, D.T. Jost, M. Schwikowski, A. Kasper, H. Puxbaum

Trajectory analysis of aerosol measurements at high alpine sites

B.P. M., B. P., C. T., S. W. (Eds.), Transport and Transformation of Pollutants in the Troposphere, Academic Publishing, Den Haag (1994), pp. 689-693

View Record in ScopusGoogle Scholar

Shen et al., 2011

Z. Shen, X. Wang, R. Zhang, K. Ho, J. Cao, M. Zhang

Chemical composition of water-soluble ions and carbonate estimation in spring aerosol at a semi-arid site of Tongyu, China

Aerosol Air Qual. Res., 10 (2011), pp. 360-368

View PDFCrossRefView Record in ScopusGoogle Scholar

Shubhankar and Ambade, 2016

B. Shubhankar, B. Ambade

Chemical characterization of carbonaceous carbon from industrial and semi urban site of eastern India

Spring, 5 (1) (2016), p. 837

View Record in ScopusGoogle Scholar

Sippula et al., 2009

O. Sippula, J. Hokkinen, H. Puustinen, P. Yli-Pirilä, J. Jokiniemi

Comparison of particle emissions from small heavy fuel oil and wood-fired boilers

Atmos. Environ., 43 (2009), pp. 4855-4864

ArticleDownload PDFView Record in ScopusGoogle Scholar

Squizzato and Masiol, 2015

S. Squizzato, M. Masiol

Application of meteorology-based methods to determine local and external contributions to particulate matter pollution: a case study in Venice (Italy)

Atmos. Environ., 119 (2015), pp. 69-81

ArticleDownload PDFView Record in ScopusGoogle Scholar

Stein et al., 2015

A.F. Stein, R.R. Draxler, G.D. Rolph, B.J.B. Stunder, M.D. Cohen, F. Ngan

NOAA's HYSPLIT atmospheric transport and dispersion modelling system

Bull. Am. Meteorol. Soc., 96 (2015), pp. 2059-2077

View Record in ScopusGoogle Scholar

Stohl, 1998

A. Stohl

Computation, accuracy and applications of trajectories—a review and bibliography

Atmos. Environ., 32 (6) (1998), pp. 947-966

ArticleDownload PDFView Record in ScopusGoogle Scholar

Szidat et al., 2006

S. Szidat, T.M. Jenk, H.A. Synal, M. Kalberer, L. Wacker, I. Hajdas, A. Kasper-Giebl, U. Baltensperger

Contributions of fossil fuel, biomass-burning, and biogenic emissions to carbonaceous aerosols in Zurich as traced by ^{14}C

J. Geophys. Res., 111 (2006), Article D07206

View Record in ScopusGoogle Scholar

Tositti et al., 2014

L. Tositti, E. Brattich, M. Masiol, D. Baldacci, D. Ceccato, S. Parmeggiani, M. Stracquadanio, S. Zippoli

Source apportionment of particulate matter in a large city of southeastern Po valley (Bologna, Italy)

Environ. Sci. Pollut. Res., 21 (2014), pp. 872-890

View PDFCrossRefView Record in ScopusGoogle Scholar

Velali et al., 2016

E. Velali, E. Papachristou, A. Pantazaki, T. Choli-Papadopoulou, N. Argyrou, T. Tsourouktsoglou, S. Lialiaris, A. Constantinidis, D. Lykidis, T.S. Lialiaris, A. Besis, D. Voutsa, C. Samara

Cytotoxicity and genotoxicity induced in vitro by solvent-extractable organic matter of size-segregated urban particulate matter

Environ. Pollut., 218 (2016), pp. 1350-1362

ArticleDownload PDFView Record in ScopusGoogle Scholar

Viana et al., 2006

M. Viana, X. Querol, A. Alastuey, J.I. Gil, M. Menendez

Identification of PM sources by principal component analysis (PCA) coupled with wind direction data

Chemosphere, 65 (2006), pp. 2411-2418

ArticleDownload PDFView Record in ScopusGoogle Scholar

Viana et al., 2009

M. Viana, F. Amato, A. Alastuey, X. Querol, T. Moreno, S.G. Dos Santos, M.D. Herce, R. Fernández-Patier

Chemical tracers of particulate emissions from commercial shipping

Environ. Sci. Technol., 43 (2009), pp. 7472-7477

View PDFCrossRefView Record in ScopusGoogle Scholar

Viana et al., 2014

M. Viana, J. Pey, X. Querol, A. Alastuey, F. de Leeuw, A. Lukewille

Natural sources of atmospheric aerosols influencing air quality across Europe

Sci. Total Environ., 472 (2014), pp. 825-833

ArticleDownload PDFView Record in ScopusGoogle Scholar

Watson et al., 2002

J.G. Watson, T. Zhu, J.C. Chow, J. Engelbrecht, E.M. Fujita, W.E. Wilson

Receptor modelling application framework for particle source apportionment

Chemosphere, 49 (2002), pp. 1093-1136

ArticleDownload PDFView Record in ScopusGoogle Scholar

Wedepohl, 1995

K.H. Wedepohl

The composition of the continental crust

Geochim. Cosmochim. Acta, 59 (1995), pp. 1217-1232

Google Scholar

Westgate and Wania, 2011

J.N. Westgate, F. Wania

On the construction, comparison, and variability of airsheds for interpreting semivolatile organic compounds in passively sampled air

Environ. Sci. Technol., 45 (2011), pp. 8850-8857

View PDFCrossRefView Record in ScopusGoogle Scholar

Zeng and Wang, 2011

T. Zeng, Y. Wang

Nationwide summer peaks of OC/EC ratios in the contiguous United States

Atmos. Environ., 45 (2011), pp. 578-586

ArticleDownload PDFView Record in ScopusGoogle Scholar

Zhang et al., 2008a

L. Zhang, R. Vet, A. Wiebe, C. Mihele, B. Sukloff, E. Chan, M.D. Moran, S. Iqbal

Characterisation of the size-segregated water-soluble inorganic ions at eight Canadian rural sites

Atmos. Chem. Phys., 8 (2008), pp. 7133-7151

View PDFCrossRefView Record in ScopusGoogle Scholar

Zhang et al., 2008b

R. Zhang, Z. Han, Z. Shen, J. Cao

Continuous measurement of number concentrations and elemental composition of aerosol particles for a dust storm event in Beijing

Adv. Atmos. Sci., 25 (2008), pp. 89-95

View PDFCrossRefView Record in ScopusGoogle Scholar

Zhao and Gao, 2008

Y. Zhao, Y. Gao

Acidic species and chloride depletion in coarse aerosol particles in the US east coast

Sci. Total Environ., 407 (2008), pp. 541-547

ArticleDownload PDFView Record in ScopusGoogle Scholar

Cited by (94)

- Two-year systematic investigation reveals alterations induced on chemical and bacteriome profile of PM<inf>2.5</inf> by African dust incursions to the Mediterranean atmosphere
  2022, Science of the Total Environment
  Show abstract
- Evolution of aerosol chemistry in Beijing under strong influence of anthropogenic pollutants: Composition, sources, and secondary formation of fine particulate nitrated aromatic compounds
  2022, Environmental Research
  Show abstract
- Molecular chemodiversity of water-soluble organic matter in atmospheric particulate matter and their associations with atmospheric conditions
  2022, Science of the Total Environment
  Show abstract
- Development and characterization of a gold nanoparticles glassy carbon modified electrode for dithiotreitol (DTT) detection suitable to be applied for determination of atmospheric particulate oxidative potential
  2022, Analytica Chimica Acta
  Show abstract
- Particulate matter geochemistry of a highly industrialized region in the Caribbean: Basis for future toxicological studies
  2022, Geoscience Frontiers
  Show abstract
- Contribution of anthropogenic and natural sources in PM10 during North African dust events in Southern Europe
  2021, Environmental Pollution